THE RATE OF OXIDATION OF PYRITES FROM COAL AND ORE SOURCES - AN AC IMPEDANCE STUDY[1]

S. Chander and A. Briceno[2]

Abstract.--The rate of oxidation of pyrites from coal and mineral sources has been determined using a new technique of AC impedance spectroscopy. In this technique the impedance of the pyrite/solution interface is measured as a function of frequency from which the charge transfer resistance can be calculated. From the charge transfer resistance the rate of oxidation is calculated using the Stern-Geary equation. The results show that the rate of oxidation of the pyrite sample from a coal source is substantially greater than the corresponding rate of oxidation of the pyrite sample from an ore source. The charge transfer resistance of the ore pyrite increases with the extent of oxidation whereas the coal pyrite showed no such increase. In the case of ore pyrite the surface film acts as a passivating layer and retards the rate of oxidation. The formation of a protective film on coal pyrite is not observed.

RATE OF PYRITE OXIDATION AND ACID MINE DRAINAGE

The pollution of mine waters by acids generated through oxidation of pyrite is a well recognized problem, particularly for the coal industry. Although the potential for acid mine drainage (AMD) depends on a variety of factors which include sulfide content, sulfide form, sulfide surface area, rock type (acid neutralization capacity), and rock permeability, prediction of the amount of acid generated still remains a difficult task (Caruccio 1968, Barton 1978, Rose et al. 1983). A major factor in the amount of free acid generated is the relative rates of acid generation through oxidation of the sulfide and the rate of acid consumption by the host rock. This is schematically illustrated in figure 1 in which G_1 and G_2 refer to two different rates of acid generation and C_1 and C_2 refer to two different rates of acid consumption. Clearly, the amount of acid generated, shown by the hatched area, is substantially greater for (G_1, C_1) conditions than it is for (G_2,C_2) conditions even though the total amount of sulfide is the same. Thus, one approach to decrease the AMD problem is to reduce the rate of oxidation of pyritic minerals. However, this approach requires an understanding of the factors that determine the rate of pyrite oxidation.

The importance of the rate of oxidation of pyrite in AMD has been recognized by many investigators (Singer

[1]Paper presented at the 1988 Mine Drainage and Surface Mine Reclamation Conference sponsored by the American Society for Surface Mining and Reclamation and the U.S. Department of the Interior (Bureau of Mines and Office of Surface Mining Reclamation and Enforcement), April 17-22, 1988, Pittsburgh, PA.

[2]S. Chander is Associate Professor of Mineral Processing and A. Briceno is a Graduate Assistant, Mineral Processing Section, The Pennsylvania State University, University Park, PA.

Proceedings America Society of Mining and Reclamation, 1987 pp 164-196
DOI: 10.21000/JASMR88010164

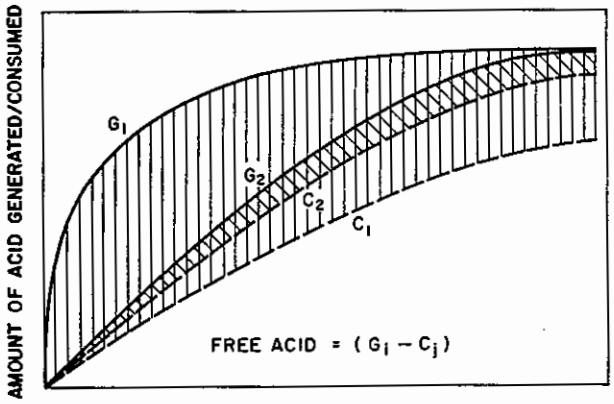

Figure 1.--A schematic representation of the amount of acid generated (G_1 or G_2) by oxidation of sulfides and the amount of acid consumed (C_1, C_2) by the host rock. The hatchured areas represent the amount of acid generated for two sets of conditions: ▥ - (G_1, C_1) and ▨ - (G_2, C_2).

and Stumm 1970, McKibben 1984), but the techniques for studying oxidation rates and the conditions of investigation vary considerably. The rates have been determined by:

1) Measurements of the amount of acid generated (represented as acidity in $CaCO_3$ equivalent);

2) Measurements of iron species in solution as Fe^{2+} and Fe^{3+};

3) Measurements of sulfur species in solution as $SO_4^{=}$, $S_xO_y^{=}$, etc;

4) Measurements of changes in pH or free H^+ concentration in solution;

5) Measurements of Eh of slurry which is a measure of Fe^{3+}/Fe^{2+}, P_{O_2}, etc. in solution;

6) Analysis of solid oxidation products (possible only when substantial fraction of pyrite has oxidized).

Although each of these techniques gives a measure of the rate of oxidation, the results cannot be directly related because pyrite oxidation occurs through formation of several intermediate ions like ferrous, ferric, thiosulfate, dithionate, etc.; and solid products like elemental sulfur, ferrous and ferric hydroxides, geothite, lepidocrocite, maghemite, and hematite. The study of the mechanism of pyrite oxidation, particularly in slightly acidic to slightly alkaline solutions, is further complicated by formation of surface coatings of the solid oxidation products. The presence of such oxidation products might change the rate limiting step from the chemical (or electrochemical) reaction

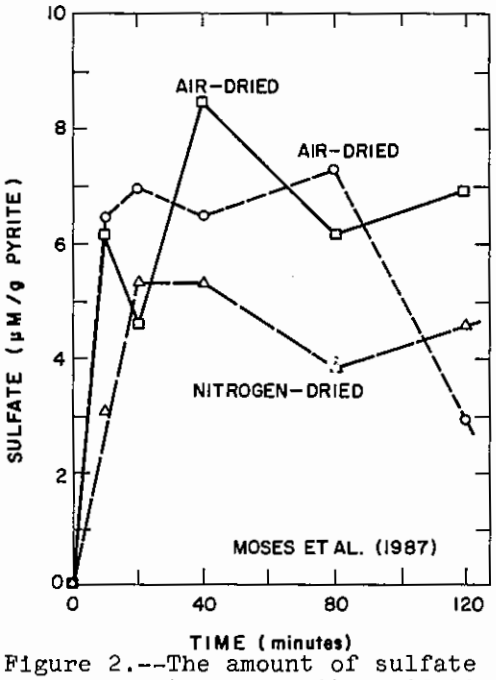

Figure 2.--The amount of sulfate generated by pyrite oxidation in oxygen-saturated solutions at initial pH 9 (Moses et al. 1987).

control to mass transfer control through the product layer. The results of pyrite oxidation reproduced in figure 2 from a recent study (Moses et al. 1987) clearly show that the data are difficult to intepret in terms of a kinetic model. Attempts by other investigators to intepret the simple kinetic data, particularly for oxidation in mild conditions have also met with difficulties (Esposito et al. 1987). This investigation was undertaken to develop a new technique of AC impedance spectroscopy to measure reactivity of the pyrite/solution interface.

AC IMPEDANCE SPECTROSCOPY

The technique of AC impedance spectroscopy to measure reactivity of pyrite is based on measurements of current through a pyrite electrode. The current is directly proportional to the rate of oxidation, which depends upon the potential, E, of the electrode (the potential represents the driving force for oxidation). If a sinusoidal potential,

$$E = \Delta E \sin \omega t$$

is applied, the current through the electrode is

$$i = \Delta i \sin (\omega t + \phi)$$

where ΔE is the amplitude of the AC signal, ω is the angular frequency ($=2\pi f$, where f is the frequency in hertz), Δi is the amplitude of the current, and ϕ is the phase lag. The impedance, Z, is defined as

$$Z = dE/dI$$

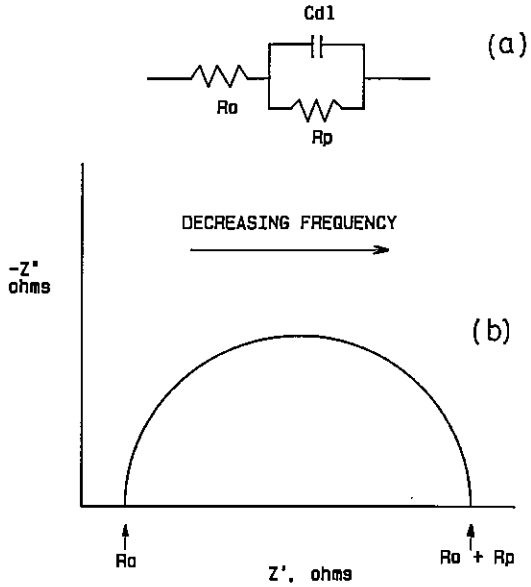

Figure 3.--a) A simple equivalent circuit for pyrite/solution interface. R_p - charge transfer resistance, C_{dl} - interfacial capacitance, and R_o - solution resistance. b) A Nyquist plot of equivalent circuit shown in figure 3a.

In general, the impedance consists of a real component, Z', and an imaginary component, Z", such that

$$Z = Z' + jZ"$$

If the pyrite/solution interface is represented by a resistance term, R, and a capacitance term, C,

$$Z' = R,$$

$$Z" = 1/(\omega C)$$

Ac impedance spectroscopy involves measurements of the impedance as a function of frequency from which the values of R and C can be obtained. A simple equivalent circuit for the pyrite/solution interface is given in Figure 3a where R_p represents the change transfer term for the pyrite/solution interface, C represents the interfacial capacitance, and R_o represents the solution resistance. The results of the impedance measurements can be plotted in the form of a Nyquist plot shown in Figure 3b from which values of R_p can be obtained. The values of R_p obtained for pyrites from different sources are discussed in this paper. The capacitances were also obtained, but will be discussed elsewhere. The rate of oxidation of pyrite, which can be represented as the exchange current density, I_o, is related to the change transfer resistance through the Stern-Geary equation

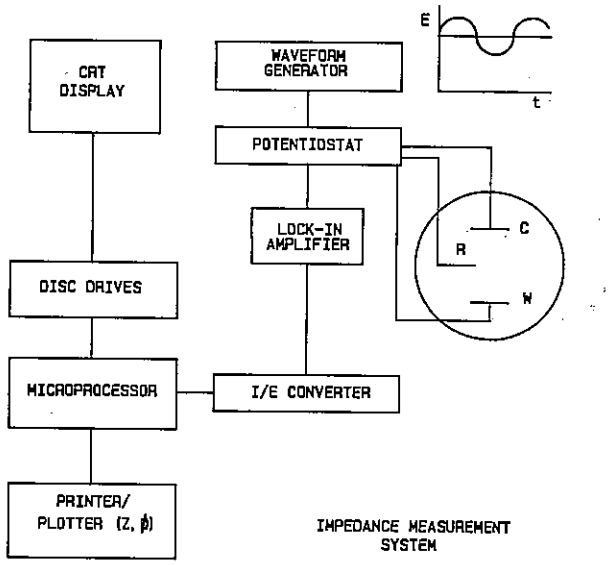

Figure 4.--A schematic of the impedance measurement system. W-working electrode (pyrite), C-counter electrode (graphite), and R-reference electrode.

$$I_o = \frac{1}{2.303R_p} \cdot \frac{b_a b_c}{b_a + b_c}$$

where b_a and b_c are the anodic and cathodic Tafel slopes, respectively.

EXPERIMENTAL METHODS AND MATERIALS

The impedance measurements were made with a Model 368-1 impedance system manufactured by EG&G Princeton Research. It consists of a Model 173 potentiostat and a Model 5706 lock-in amplifier. Both units are operated by an Apple IIe microcomputer through a Model 276 interface. Both the data acquisition and analysis were carried out with the aid of the computer. A typical impedance experiment consisted of the measurement of the magnitude and phase angle of the impedance as a function of frequency. An AC signal of 10_4mV in the frequency range of 10^{-3} to $2x10^4$ Hz was used in the impedance measurements. A schematic of the electrochemical setup is shown in figure 4. A three-electrode system was used in which the working electrode was a polished specimen of pyrite of 1 cm^2 geometric area. A saturated calomel electrode was used as the reference electrode and two graphite rods were used as the counter electrodes.

The pyrite crystals were cut to size, and the exposed surface of the sample was polished on a 600-grit silicon carbide paper. The samples were polished wet under distilled water and then trans-

ferred to the cell quickly after washing. Samples were handled only by gloves during the entire polishing procedure. Although pyrite oxidation could not be prevented by this procedure, alternate chemical treatments were found to be unsatisfactory. The solution was deoxygenated by bubbling purified nitrogen overnight before inserting the sample in the cell. Nitrogen was bubbled throughout the conditioning period, which lasted about three hours unless otherwise stated. During an electrochemical measurement, the flow of nitrogen at the surface of the solution was continued to eliminate diffusion of atmospheric oxygen into the cell.

The ore pyrite sample was from Muro de Aguas, Logrono Province, Spain, and the coal pyrite was from a "sulfur ball" from the Lower Kittaning Seam, PA.

Distilled water from a tin-lined Barnstead still (Model 210) equipped with a Q-baffle system was used in this investigation. Water of specific resistivity greater than 2 Mohm-cm was used in all the experiments, which were conducted at room temperature.

RESULTS AND DISCUSSION

The results of the AC impedance measurements for the coal and ore pyrite samples are presented in figure 5. The charge transfer resistance (R_p) is plotted as a function of the DC potential for the pyrite/solution interface. It is small when the electrochemical reactivity of the interface is large (i.e., large reaction rate) and vice-versa. The results in figure 5 show that the coal pyrite is generally more reactive than the mineral pyrite in the potential range of -0.4 to 0.4 V. The functional dependance of the charge transfer resistance on potential is also different for the two pyrites. The ore pyrite sample shows a maximum in R_p at 0.25 V*. This potential is slightly greater than the rest potential of pyrite, which is 0.19 V. In contrast to this behavior, the coal pyrite shows a maximum in the charge transfer resistance at 0.12 V, which is slightly below the rest potential of coal pyrite (0.28 V). The magnitude of the charge transfer resistance for this pyrite is about 25 times smaller than the corresponding value for the ore pyrite. These results imply that the coal pyrite begins to

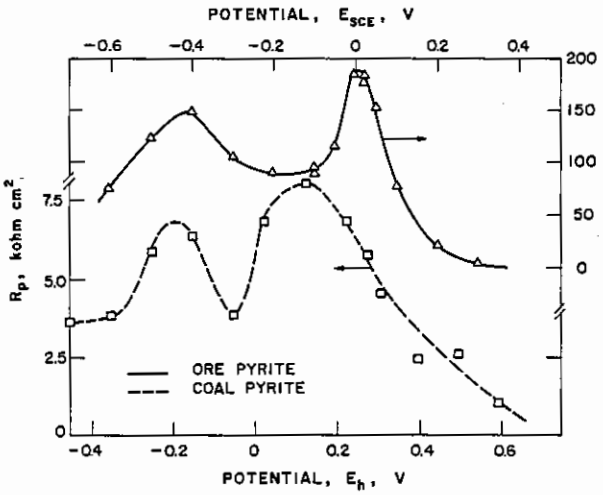

Figure 5.--The charge transfer resistance for an ore and a coal pyrite as a function of the DC potential.

oxidize at lower potentials than ore pyrite. The exchange current densities obtained by using the Stern-Geary equation are plotted in figure 6 for the pyrites from the coal and the ore sources. The high reactivity of the coal pyrite is clearly seen. The filled symbols are the exchange current densities obtained by steady state polarization measurements.

For the ore pyrite, the charge transfer resistance increases with increase in the extent of reaction as shown in figure 7, in which R_p is plotted as a function of charge transferred. In this series of tests, an anodic charge was passed to oxidize the pyrite under galvanostatic conditions (i.e. constant rate of oxidation), and the AC impedance measurements were carried out after a predetermined amount of charge was passed. The increase in R_p for the ore pyrite shows that a film forms on the surface of pyrite, the resistance of which increases with the amount of charge transferred or extent of the reaction. The film acts as a passivating layer and retards the rate of oxidation. A passivating film does not form on the surface of the coal pyrite, however. The results for coal pyrite, in figure 7, show that the charge transfer resistance does not increase with charge transferred. The coal pyrite continues to oxidize rapidly due to the absence of a protective film.

The nature of product layers on the surface of the reacted pyrites can be schematically represented as shown in figure 8. The product layer is relatively nonporous (or dense) at the surface of the ore pyrite (fig. 8a), whereas it is highly porous at the surface of the coal pyrite (fig. 8b).

*The impedance measurements on ore samples from alternate sources show a similar behavior with the exception that the magnitude of the charge transfer resistance is different for each pyrite. The charge transfer resistance correlates very well with the oxidation behavior also. These results are published elsewhere (Chander and Briceno 1987).

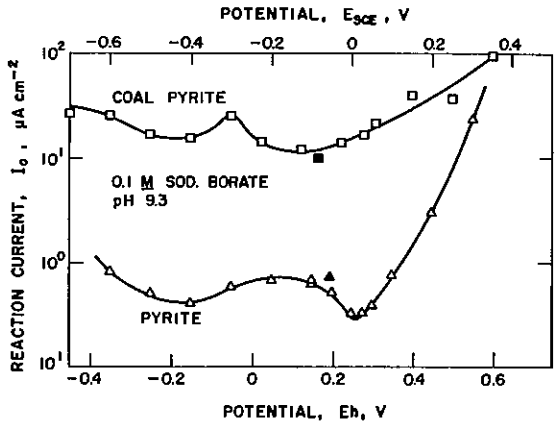

Figure 6.--The reactivities of pyrites from two different sources as a function of the DC potential.

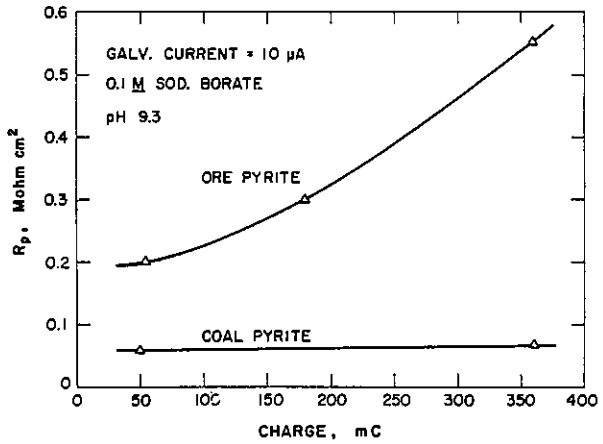

Figure 7.--The charge transfer resistance of ore and coal pyrites as a function of the extent of reaction (measured in terms of charge transferred).

Further analysis of the impedance data with the aid of a two-layer model (Chander et al. 1988) shows that the resistance of the coal pyrite/solution interface is primarily a charge transfer resistance (i.e., resistance of the porous film is negligible), whereas the resistance of the ore pyrite/solution interface consists of a charge transfer term for the product layer. Although the reasons for formation of a passivating film on the ore pyrite or the lack of a passivating film on the coal pyrite are not entirely clear, it is believed that the micropores in coal pyrite play an important role. For coal pyrite the dissolution occurs inside the pores or microcracks whereas precipitation of the product occurs outside the mouth of the micropore or crack. The product layer is sufficiently porous to allow diffusion of reactants and products. The conditions

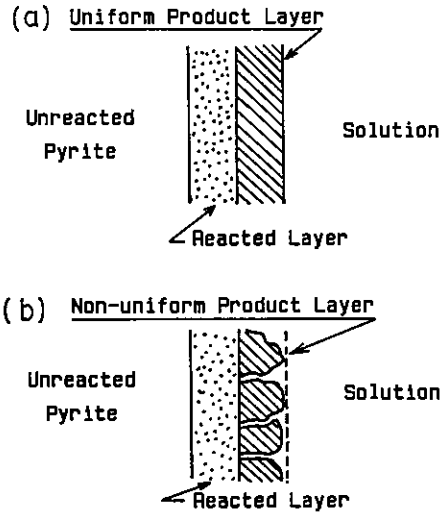

Figure 8.--A schematic representation of surface layers on pyrite.

which give rise to a change in the characteristics of the product layer can significantly alter the rate of pyrite oxidation. Additional studies are needed to determine the nature of surface films that form on the surface of pyrites and the role they play in pyrite oxidation phenomena.

SUMMARY

A new technique of AC impedance spectroscopy has been developed to determine the rate of oxidation of pyrite. This technique is especially useful for studying the reactivity of solids when product layers form at the interface. The study of oxidation of an ore pyrite, which is a hydrothermal pyrite, shows that a protective film forms on the surface of pyrite which retards the rate of reaction. In contrast, the microporous nature of coal pyrite, which is a brackish-water pyrite, gives rise to a nonproductive (highly porous) product layer.

ACKNOWLEDGEMENTS

The authors acknowledge the financial assistance from the National Science Foundation under grant, MSM-8413477 and the U.S. Department of Energy under grant No. DE-FG22-85 PC80523 in support of this research.

LITERATURE CITED

Barton, P. 1978, The acid mine drainage In Sulfur in the environment, Pt. II, Ecological Impacts. J.O. Nriagu (Ed.), Wiley, New York, NY, pp. 313-358.

Caruccio, F.T., 1968, An evaluation of factors affecting acid mine drainage production and the ground water interactions in selected mine areas of Western Pennsylvania In Second Symposium on Coal Mine Drainage Research, Monroeville, PA, pp. 107-152.

Chander, S. and Briceno, A., 1987, Kinetics of pyrite oxidation. Minerals and Metallurgical Processing, 4:171-176.

Chander, S., Pang, J. and Briceno, A., 1988, A two layer model for AC impedance analysis of pyrite/solution interface to be presented at the Symposium on Electrochemistry in Mineral and Metal Processing, the Electrochemical Society, Atlanta, GA, May 15-20.

Esposito, M.C., Chander, S. and Aplan, F.F., 1987, Characterization of pyrite from coal sources In Process Mineralogy VII. A.H. Vansiliou (Ed.). TMS/AIME, in press.

McKibben, M.A., 1984, Kinetics of aqueous oxidation of pyrite by ferric iron, oxygen and hydrogen peroxide from pH 1-4 and 20-40°C. Ph.D. Thesis. The Pennsylvania State University, 159 pp.

Moses, C.O., Nordstrom, D.K., Herman, J.S. and Mills, A.L., 1987, Aqueous pyrite oxidation by dissolved oxygen and ferric iron. Geochimica et Cosmochimica Acta. 51:1561-1571. http://dx.doi.org/10.1016/0016-7037(87)90337-1

Rose, A. W., Williams, E. G., and Parizek, R. B., 1983, Predicting potential for acid mine drainage from coal mines. Earth and Mineral Sciences Bull., The Pennsylvania State University 52:37-41.

Singer, P.C. and Stumm, W., 1970, Acid mine drainage: The rate limiting step. Science. 167:1121-23. http://dx.doi.org/10.1126/science.167.3921.1121